Observation of Two-dimensional Branched Flow of Light

Ke Lin,[1,2] Zhaoyu Liu,[1,2] Jianwei Qin,[2] Qidong Fu,[2] Peng Wang,[2,*] and Fangwei Ye[2,†]

[1] *Zhiyuan College, Shanghai Jiao Tong University, Shanghai 200240, China*
[2] *School of Physics and Astronomy, Shanghai Jiao Tong University, Shanghai 200240, China*

(Dated: May 17, 2023)

We present an experimental study on light propagation in a bulk material, in which a weakly disordered, three-dimensional spatial fluctuation of refractive index is induced in a controlled way. We demonstrate the first observation of the stable two-dimensional branched flow of light and experimentally identify the fundamental length scale at which the two-dimensional branching starts. We find that the scintillation index can be applied to the three-dimensional wave flow and that its peak value corresponds to the formation of distinct network of surface caustics that are interconnected. Influence of transverse anisotropy of the disordered potential on the light branching are reported too. The observed branching properties are in excellent agreement with theoretical analyses based on the paraxial light-propagation equation.

Introduction.—When a wave propagates through a smooth, disordered potential with a correlation length longer than its wavelength, it divides into channels (branches) of enhanced intensity and keep dividing as they propagate. This tree-like beautiful phenomenon is known as branched flow. It was first observed in the flow of electrons in two-dimensional electron gases(2DEGS) [1, 2], where the stability [3, 4], statistics property [5–7], behaviors in anisotropic media [8], and pattern shaping [9] of the branched flows are studied. Due to its nature of wave, branch flows are found to occur in diverse systems, such as shallow water waves [10], relativistic particles [11], microwaves in a resonator [12, 13], and even the structure of our universe [14].

Very recently, branched flow of light was observed for the first time when a laser beam propagating inside a soap film [15], and followed by the observation of branched flow of light in curved space [16] and branched flow of incoherent light [17]. Similar to its initial experimental observation in 2DEGs, the study of the branch flows in a soap film, or in other systems has predominantly focused on (1+1)-dimensional (D) cases, where one dimension is transversal and undergoes diffraction(branching), while the other is longitudinal and undergoes evolution. However, branched flow phenomena occur not only in (1+1)D wave systems but also in (2+1)D systems, whereby wave branching can take place in any direction of the transverse plane, providing a much more rich branching dynamic than in (1+1)D wave systems. Despite some theoretical proposals on (2+1)D branching dynamics [14, 18], an experimental observation of 2D branched flow of light (or any waves) is still missing.

Here, we report the first observation of stable branched flow of 3D wave fields by propagating a laser beam in a bulk, photorefractive crystal into which a purpose-designed 3D weakly disordered potential is embedded. We find that the scintillation index reaches its peak value at a evolution distance at which a broad light beam evolves into a network of interconnected caustic surfaces with distinct intensity peaks and 2D light branching occurs. We thus identify the fundamental length scale d_0 associated with weak, correlated (2+1)D random media that marks the onset of branching. We also find that the transversal anistropic in correlation of the disorder potentials significantly alters the direction into which the light branching occurs. Our experimental observations on (2+1) branching is well supported by the direct simulation of light propagation based on the paraxial light-propagation equation.

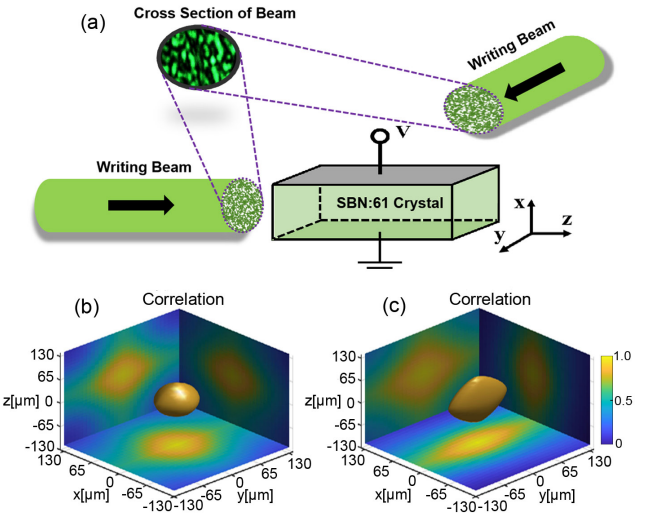

FIG. 1. (a) Experimental scheme for laser-writing photonic Gaussian random potential into a SBN:61 crystal. (b) Isotropic ($l_x = l_y = l_z = l_c = 98\mu$m), and (c) anisotropic ($l_x = 62\mu\text{m}, l_y = l_z = 147\mu$m) correlation function of the experimentally induced 3D random potential.

Experimental scheme in inducing 3D disorder potentials.—We employ the optical induction technique [19–21] to generate a 3D random potential, $V(x, y, z)$, in a crystal of Strontium-barium niobate (SBN:61). To accomplish this, we utilize two speckled beams obtained from diffusers to "write" disorder into

the sample (see Figure 1 for the experimental scheme and [22] for details): one beam enters from the front facet of the sample, generating a disordered potential $V_1(x, y)$ in the transverse plane (xy) [invariant in the longitudinal direction z]; the other beam enters the crystal laterally, creating a disorder potential $V_2(x, z)$ in the plane (xz) [invariant in the direction y]. Since the two "writing" beams are incoherent each other, the resulting disorder potentials are simply superimposed in the bulk of the sample, creating the desired 3D potential $V(x, y, z) = V_1(x, y) + V_2(x, z)$.

To characterize the resulting random potential V, we use the spatial auto-correlation function $f_c(\mathbf{r})$ [$\mathbf{r}$=(x, y, z)] which we choose to be Gaussian with width l_i $(i = x, y, z)$ and amplitude σ, [23]

$$f_c(\delta\mathbf{r}) = \langle V(\mathbf{r})V(\mathbf{r}+\delta\mathbf{r})\rangle = \sigma^2 \exp[-(\frac{\delta x^2}{2l_x^2} + \frac{\delta y^2}{2l_y^2} + \frac{\Delta z^2}{2l_z^2})] \quad (1)$$

Figures 1(b) and (c) presents two examples of auto-correlation function $f_c(\mathbf{r})$, fitted from two specific realizations of disorder potential prepared in our experiments. By controlling the size and the aspect ratio of two writing speckled beams, we can readily achieve various disorder potentials with controlled correlation lengths [22], including isotropic [$l_x = l_y = l_z$, Fig. 1 (b)] and anisotropic [$l_x \neq l_y$, Fig. 1(c)] ones. Thus, the stability and controllability of disorders generated in this manner is opposed to the time-varying disorders in a liquid membrane [15]. On the other hand, the intensity of the writing beam and the applied biasing voltage across the sample are fixed to be 3.93 mW/cm^2 and 800 V respectively, resulting into a strength of the disorder potential $\sigma \sim 10^{-3}$(corresponding to a change of refractive index $\delta n \sim (2 \sim 3) \times 10^{-4}$). This relative weak strength of the disorder, together with its long correlation length, indeed meet the criteria necessary for branched flow to occur, as will be shown below.

Experimental observation of 2D branched flows of light.—We initial our study by experimenting with the propagation of light in isotropic disorder potential (as shown in Figure 1(b)). A probe light, a 633-nm laser beam, was expanded to a width of 8 mm and directed towards the disordered-imprinted SBN:61 crystal with a transverse dimension 5 × 5 mm^2 and length of 20 mm, effectively mimicking a plane wave excitation. Interestingly, the plane wave, subject to the smooth perturbation of the underlying disorder, resulting in the formation of a network of caustic surfaces where the light is strongly concentrated, leaving their surrounded spatial regions relative dark. The caustic surfaces are interconnected through "hot spots" of intensity peaks (as shown Fig. 2(b,i)), where strong two-dimensional localization of light occur. The two-dimensional caustic networks remain structurally stable for a considerable distance, with more energy being pumped from the darker regions until

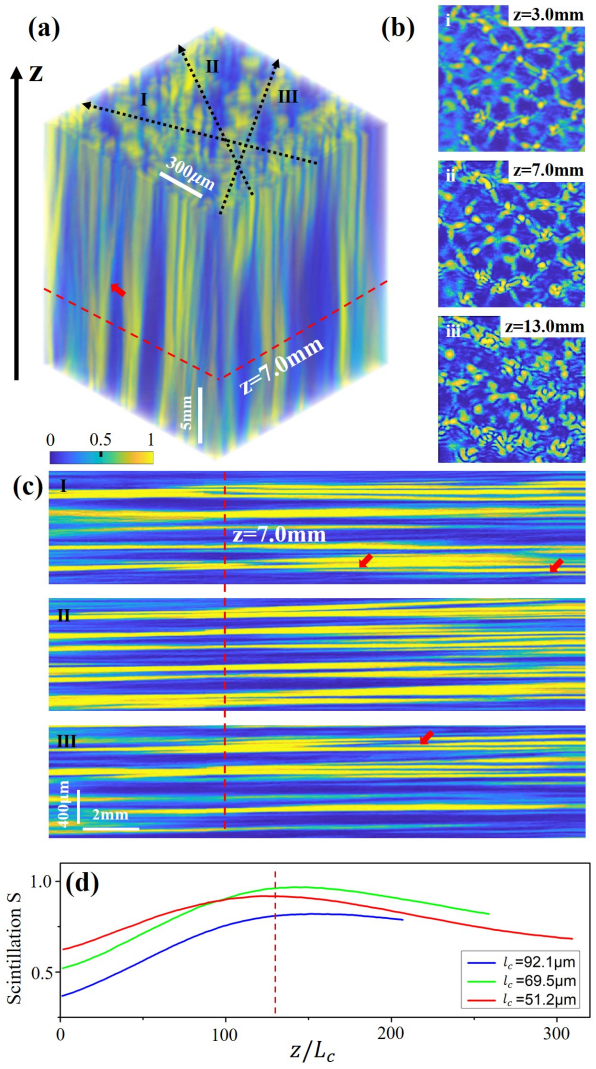

FIG. 2. Experimental observation of branched flows. (a) (2+1)D branched flow of light. (b) Light intensity distribution on transverse planes at three propagation distances z. (c) Light intensity distribution on three arbitrarily selected slices along the z axis. The orientation of the slices are indicated by the dashed lines in (a). (d) Scintillation index S as a function of the normalized distance z/l_c, for light propagation in disorder potentials with three different correlation lengths. The red dashed lines in (a),(c) and (d) mark the position where the scintillation index achieves it peak value. Red arrows in (a) and (c) indicate the positions where light branching continues after the first instance of branching.

the hot spots become strong enough to branch out (as shown in Fig. 2(b,ii)), followed closely by branching from the caustic sheets between the hot spots. It is important to emphasize that the branching flow occurs extensively throughout the entire volume of the light beam, as evident from the two side faces of the 3D wave field (as shown in Figure 2(a)) and three arbitrarily selected slices along the longitudinal axis z (as shown in Figure

2(c)). This wide-spreading light branching leads to the gradual development of the caustic networks into a granular speckle pattern with propagation distance, as shown in the bottom panel of Figure 2(b). Also note that, after the first instance of light branching, there continues to be branching at various points, such as the positions indicated by the red arrows in Fig. 2.

It is widely recognized that the fundamental properties of branched flow are independent of the specific details of disorder potentials and the propagation dynamics of the wave field. Instead, they solely depend on two parameters that characterize the disorder potentials - the correlation length l_c and the strength of the perturbation σ. Thus, the average distance from the source to the first branching point, d_0, is given by $d_0 = \alpha l_c \sigma^{-2/3}$ [5, 24, 25], where α is a proportionality factor that is determined by the form of the correlation function and system's dimension [24]. In our laser-writing scheme, we are capable of generating photonic disorder potentials with desired values of l_c and σ, which facilitates the study of their relationship with d_0. To determine d_0 from the experimental data, we utilize the scintillation index, $S(z) = \langle I^2(\mathbf{r}_\perp, z)\rangle / \langle I(\mathbf{r}_\perp, z)\rangle^2 - 1$, which measures the average variance of the intensity distribution, scaled by the square of the mean intensity - as a function of distance z. Here, $\langle f(\mathbf{r}_\perp, z)\rangle$ represents the ensemble average of the quantity f over many different disorder potentials with the same σ and l_c. The scintillation index is widely used to identify the onset of the first branching point, where it exhibits a peak.

The evolution of scintillation index S with propagation distance z, as extracted from the experimental data, is given in Fig. 2(d) for three different correlation lengths l_c (but with the same σ). Here, for each correlation length, the scintillation index is obtained after averaging over 20 specific realizations of disorders. As shown in Fig. 2(d), with the propagation distance, the scintillation index first progressively increases, corresponding to the steady formation of the caustic structures (Fig. 2(b,i)), and then reaches a peak value at a distance where the 2D caustic networks evolve into the most distinct pattern (i.e., the sharpest) and the onset of the 2D branching occurs (Fig. 2(b, ii)). Thereafter, the scintillation index decreases monotonically with distance z. Thus, in contrast to 1D branching, where the scintillation index reaches its maximum when light concentrates into discrete curves, in two-dimensional branching, the maximum scintillation index occurs when light concentrates into rather interconnected caustic surface. Remarkably, we observed that the peak values of the scintillation index are all achieved at a distance z that is nicely proportional to the correlation length l_c. Thus, our experimental results clearly reveal for the first time the fundamental length scale d_0 which marks the onset of branching in weak, correlated 3D random media.

Simulation on 2D branched flows of light.—The experimentally observed branching scenarios reported above are well supported by direct simulations of a two-dimensional light beam propagating in a photorefractive medium with a weak random potential landscape. The simulation is based on the paraxial light-propagation equation of the dimensionless field amplitude, $\psi(X, Y, Z)$:

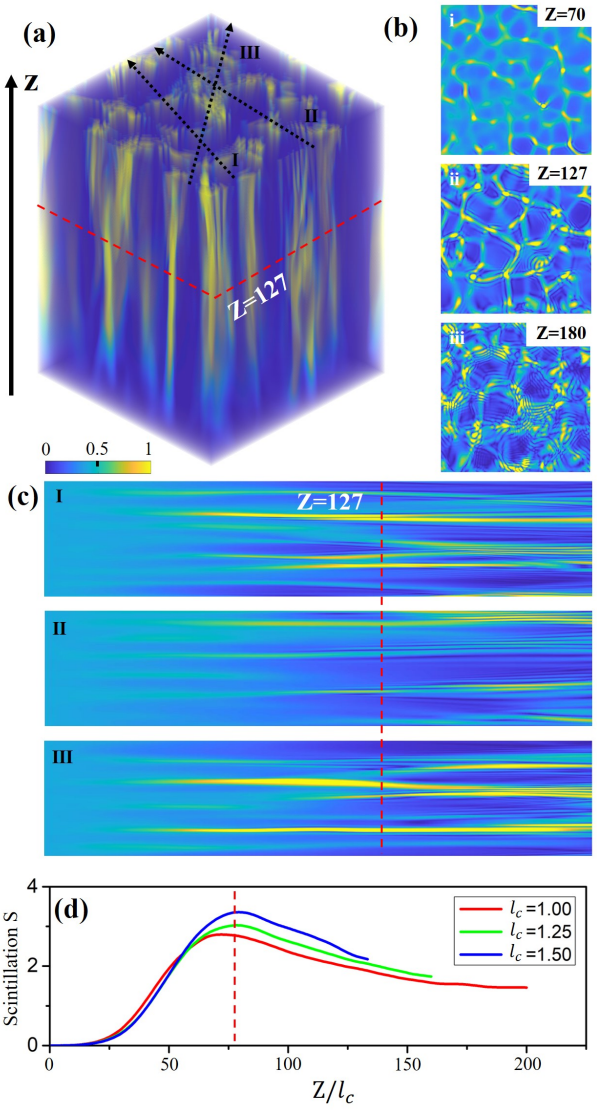

FIG. 3. Simulated results of branched flows. (a) (2+1)D branched flow of light. (b) Light intensity distribution on transverse planes at three propagation distances Z. (c) Light intensity distribution on three arbitrarily selected slices along the Z axis. The orientation of the slices are indicated by the dashed lines in (a). (d) Scintillation index S as a function of the normalized distance Z/l_c, for light propagation in disorder potentials with three different correlation lengths. For each l_c, the scintillation index S is averaged over 20 realizations of disorders. The red dashed lines in (a),(c) and (d) mark the position where the scintillation index achieves it peak value. $E_0 = 800$ is used in the simulations.

$$\mathrm{i}\frac{\partial\psi}{\partial Z} = -\frac{1}{2}\nabla_\perp^2\psi - \Delta n\psi \tag{2}$$

Here $\nabla_\perp = (\partial/\partial X, \partial/\partial Y)$; Z is the propagation distance; $\Delta n(X,Y,Z) = E_0/(1+I(X,Y,Z))$ is the refractive index change (proportional to V discussed previously); $E_0 > 0$ is the dimensionless applied d.c. field. $I(X,Y,Z)$ is the normalized intensity of the speckled writing beam, and the form in which it enters equation 2 is determined by the mechanism of the photorefractive response.

The simulation results are summarized in Fig. 3, where a plane light wave was assumed to propagate over an isotropic disorder potential with the fixed dimensionless strength $\sigma = 2.4$ (the correlation length l_c may vary from case to case, though). Figure 3 displays a 3D light wave field, together with its projection on the transversal and longitudinal slices as well as the evolution of scintillation index versus Z. The arrangement in Fig. 3 aligns with the experimental results in Fig. 2, enabling a one-to-one comparison. Although the simulation shows a distinct network of caustics that are even more pronounced than the one observed in experiments (cf. Fig 3(b, ii) and Fig 2(b, ii)), there are excellent qualitative agreements between the experimental and simulated outcomes. Note also that the scintillation index proves to a reliable measure to assess the focusing distance and the onset of branching of (2+1)D wave flows.

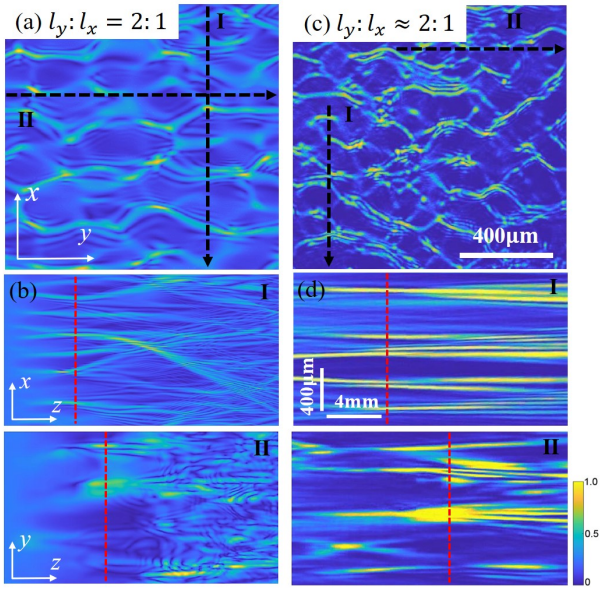

FIG. 4. (2+1)D branched flow of light in correlation anisotropic media with $l_y \neq l_x$, for simulation (a, b) ($l_x = 1, l_y = 2$) and experimental ($l_x = 62$ μm, $l_y = 147$ μm) (c, d) results. (a, c) The transversal light intensity at $Z = 86$ (a) and $z = 9.6$mm (c). (b, d) The light intensity on the xz and yz planes, whose orientations are indicated with black dashed lines in panels (a, c). The first branching on each individual plane is marked with dashed red lines.

Transverse anisotropic disorders.—As mentioned before, our approach to inducing disorder potential in photorefractive crystals offers flexibility in creating different potential landscapes, including those with transverse anisotropy(Fig. 1(c)). While previous studies have examined the effects of anisotropy on branched flow in relation to the interplay between transverse and longitudinal correction in a (1+1)D wave system [8], the (2+1)D nature of our wave system enables us to study transverse anisotropic disorders, i.e., for disorder potentials with $l_y \neq l_x$.

The results of light propagation through transverse anisotropic disorder potentials, with $l_y \approx 2l_x$, are presented in Fig. 4, consisting of both simulation (left column) and experimental (right column) data. Panels (a) and (c) display the light intensity distributions on the transverse plane at a distance z, where the overall scintillation index reaches a maximum. While there are also apparent networks of caustic surfaces as in isotropic cases, in this case, the surfaces predominantly extend along the y direction with a larger correlation, while the pattern exhibits sharp features along the x direction with a shorter correlation. This anisotropic pattern is attributed to the strong focusing effect of short correlation l_x on the broad light beam, which leads to earlier focusing of light in the x direction than in the y direction. Consequently, the light branching becomes clearly direction-dependent: it branches out predominantly in the x direction and much earlier than in the y direction, as shown in Fig. 4(b) and (d). It should be noted that in the limit case where $l_y/l_x \to \infty$, the branching in the y direction vanishes, and the system effectively recovers to the (1+1)D regime. Therefore, our anisotropic disordered potential provides a method to investigate the crossover from (2+1)D branching into (1+1)D branching.

Conclusion.—We conducted an experimental study on light propagation within a bulk material by inducing a controlled, weakly disordered, three-dimensional spatial fluctuation of refractive index. Our study demonstrates the first observation of stable two-dimensional branched flow of light and identifies the fundamental length scale at which two-dimensional branching begins. We also find that the scintillation index can be applied to three-dimensional wave flow and that its peak value corresponds to the formation of a distinct network of interconnected surface caustics. We also observed that the transversal anisotropy in the correlation of the three-dimensional disorders significantly alters the direction to which the branching occurs. The observed branching properties align closely with theoretical analyses based on the paraxial light-propagation equation.

The stable, and three-dimensional nature of the observed branched flow within the bulk material presents significant opportunities for further and full investigations into the interaction of light with weakly disordered materials. One potential research direction is the manip-

ulation and engineering of channeling of two-dimensional, localized light beams in defect-free optical structures and under pure linear conditions [9]. It is also possible to study through our experiments the impacts of structurally complex light beams, such as vectorially polarized and topologically nontrivial beams (e.g., with vortical phase structures), on the formation of branched flows. Moreover, the inherent nonlinear nature of photorefractive crystals, which accommodates the disorder potential, enables us to explore the intriguing interplay between branched flow and nonlinear optical response. This interplay includes the possibility of self-routing of spatial optical solitons in (2+1)D space and their nonlinearity-controlled steering, which are all within the experimental reaching.

* Corresponding author: lingwoxing@sjtu.edu.cn
† Corresponding author: fangweiye@sjtu.edu.cn

[1] M. A. Topinka, B. J. LeRoy, R. M. Westervelt, S. E. J. Shaw, R. Fleischmann, E. J. Heller, K. D. Maranowski, and A. C. Gossard, Coherent branched flow in a two-dimensional electron gas, Nature **410**, 183 (2001).
[2] M. A. Topinka, R. M. Westervelt, and E. J. Heller, Imaging Electron Flow, Physics Today **56**, 47 (2003), publisher: American Institute of Physics.
[3] M. P. Jura, M. A. Topinka, L. Urban, A. Yazdani, H. Shtrikman, L. N. Pfeiffer, K. W. West, and D. Goldhaber-Gordon, Unexpected features of branched flow through high-mobility two-dimensional electron gases, Nature Physics **3**, 841 (2007).
[4] B. Liu and E. J. Heller, Stability of Branched Flow from a Quantum Point Contact, Physical Review Letters **111**, 236804 (2013).
[5] L. Kaplan, Statistics of Branched Flow in a Weak Correlated Random Potential, Physical Review Letters **89**, 184103 (2002).
[6] J. J. Metzger, R. Fleischmann, and T. Geisel, Universal Statistics of Branched Flows, Physical Review Letters **105**, 020601 (2010).
[7] J. J. Metzger, R. Fleischmann, and T. Geisel, Statistics of Extreme Waves in Random Media, Physical Review Letters **112**, 203903 (2014).
[8] H. Degueldre, J. J. Metzger, E. Schultheis, and R. Fleischmann, Channeling of Branched Flow in Weakly Scattering Anisotropic Media, Physical Review Letters **118**, 024301 (2017).
[9] A. Brandstötter, A. Girschik, P. Ambichl, and S. Rotter, Shaping the branched flow of light through disordered media, Proceedings of the National Academy of Sciences **116**, 13260 (2019).
[10] H. Degueldre, J. J. Metzger, T. Geisel, and R. Fleischmann, Random focusing of tsunami waves, Nature Physics **12**, 259 (2016).
[11] M. Mattheakis, G. P. Tsironis, and E. Kaxiras, Emergence and dynamical properties of stochastic branching in the electronic flows of disordered Dirac solids, Europhysics Letters **122**, 27003 (2018).
[12] R. Höhmann, U. Kuhl, H.-J. Stöckmann, L. Kaplan, and E. J. Heller, Freak Waves in the Linear Regime: A Microwave Study, Physical Review Letters **104**, 093901 (2010).
[13] S. Barkhofen, J. J. Metzger, R. Fleischmann, U. Kuhl, and H.-J. Stöckmann, Experimental Observation of a Fundamental Length Scale of Waves in Random Media, Physical Review Letters **111**, 183902 (2013).
[14] E. J. Heller, R. Fleischmann, and T. Kramer, Branched flow, Physics Today **74**, 44 (2021).
[15] A. Patsyk, U. Sivan, M. Segev, and M. A. Bandres, Observation of branched flow of light, Nature **583**, 60 (2020).
[16] A. Patsyk, Y. Sharabi, U. Sivan, and M. Segev, Branched Flow of Light in Curved Space, in *Conference on Lasers and Electro-Optics (2022), paper FW5D.1* (2022) p. FW5D.1.
[17] A. Patsyk, Y. Sharabi, U. Sivan, and M. Segev, Incoherent Branched Flow of Light, Physical Review X **12**, 021007 (2022).
[18] G. Green and R. Fleischmann, Branched flow and caustics in nonlinear waves, New Journal of Physics **21**, 083020 (2019).
[19] N. K. Efremidis, S. Sears, D. N. Christodoulides, J. W. Fleischer, and M. Segev, Discrete solitons in photorefractive optically induced photonic lattices, Physical Review E **66**, 046602 (2002).
[20] T. Schwartz, G. Bartal, S. Fishman, and M. Segev, Transport and Anderson localization in disordered two-dimensional photonic lattices, Nature **446**, 52 (2007).
[21] L. Levi, M. Rechtsman, B. Freedman, T. Schwartz, O. Manela, and M. Segev, Disorder-Enhanced Transport in Photonic Quasicrystals, Science **332**, 1541 (2011).
[22] See the experimental setup, and the details of the controllable experimental generation of three-dimensional photonic Gaussian random potentials in a photorefractive crystal in the Supplementary Material.
[23] M. S. Simon, J. M. Sancho, and A. M. Lacasta, On generating random potentials, Fluctuation and Noise Letters **11**, 1250026 (2012).
[24] V. I. Klyatskin, Caustics in random media, Waves in Random Media **3**, 93 (1993).
[25] J. Metzger, Branched Flow and Caustics in Two-Dimensional Random Potentials and Magnetic Fields (2010).
[26] N. Akhmediev, J. M. Soto-Crespo, and A. Ankiewicz, Extreme waves that appear from nowhere: On the nature of rogue waves, Physics Letters A **373**, 2137 (2009).
[27] J. M. Dudley, F. Dias, M. Erkintalo, and G. Genty, Instabilities, breathers and rogue waves in optics, Nature Photonics **8**, 755 (2014).
[28] P. W. Anderson, Absence of Diffusion in Certain Random Lattices, Physical Review **109**, 1492 (1958), publisher: American Physical Society.